Transactions of the Korean Nuclear Society Spring Meeting
Jeju, Korea, May 22-23, 2025

Temperature influence on microstructural evolution at joining interface of Inconel 718 and 316L powders using Spark Plasma Sintering (SPS)

Seong Gyu Chung [1, a], Omer Cakmak [b], Jung Wook Cho [a,b], Kumar Sridharan [c], Hwasung Yeom [a,b*],

[a] *Graduate Institute of Ferrous & Eco Materials Technology (GIFT), POSTECH, Republic of Korea*
[b] *Division of Advanced Nuclear Engineering (DANE), POSTECH, Republic of Korea*
[c] *Department of Nuclear Engineering and Engineering Physics, University of Wisconsin Madison, WI, USA*
[*] *Corresponding author: Hwasung Yeom, hyeom@postech.ac.kr*

***Keywords:** Spark Plasma Sintering (SPS), Powder Metallurgy, Multiple Alloy System Sintering, Grain Growth Mechanism

1. Introduction

Inconel 718 is a nickel-based superalloy with chromium, iron, and titanium, showing excellent performance in high temperatures so that most of its properties including tensile strength maintain under nuclear reactor operating temperature [1, 2]. Therefore, the excellent properties of Inconel 718 allow application to structural material for various components in current and future nuclear power plants. As a precipitation hardening superalloy, Inconel 718 matrix has uniformly dispersed precipitates of FCC γ' $Ni_3(Al\ Ti)$ and BCT γ" (Ni_3Nb) phases through post heat-treatment [3, 4].

316L austenitic stainless steel has a wide application to industries. The alloy processes excellent corrosion resistance and structural properties [5, 6]. Moreover, stainless steel was used in structural components in light-water reactors and fast breeder reactors [7].

The joining of these two dissimilar alloy systems becomes essential for Generation IV reactors, as well as other industries with harsh environments [8, 9]. There are recent studies to manufacture both alloys with additive manufacturing in mesoscale; directed energy deposition (DED) and microscale laser powder bed fusion(L-PBF) [10].

Conventional manufacturing methods often face difficulties in processing Inconel 718 components as they have relatively high hardness and low thermal conductivity due to the Laves C14 phase's brittle nature. Crack formation between the joint structure of Inconel 718 and 316L was reported as a major issue under operation cycle and fatigue. Thus, brazing and hot isotactic pressing (HIP) were only cases that have been used to bond Inconel 718 and 316L.

The research presented herein focuses on manufacturing Inconel 718-Stainless steel 316L joints using spark plasma sintering process. The interfacial stability and phase evolution of each material at different temperatures have been characterized.

2. Methods and Results

2.1 Powder Compositions

Both Inconel 718 powder and 316L stainless steel powders were prepared from MK Powder.Co (South Korea). Powders' size distribution was 15 ~ 45 µm where the powder shape was spherical produced using gas atomization under industrial argon gas. Each of the alloy compositions are as follows:

Table 1: Powder Composition of IN718 and 316L Powders

Alloy Elements	IN 718	316L
Ni	50 ~ 55	11 ~ 14
Cr	17 ~ 21	16 ~ 18
Fe	19 ~ 22	Bal
Co	<1	0
Nb	4.75 ~ 5.5	0
Mo	2.8 ~ 3.3	2 ~ 3
Ti	1.15	0
Al	0.2 ~ 0.8	0
Mn	0.35	<2
Si	0.35	<1
C	0.08	0.03
Cu	0.3	0
P	0	<0.04
Si	0	<0.04

***(Wt. %)**

2.2 Spark Plasma Sintering Process

Spark plasma sintering (SPS) process is a powder consolidation technology in solid-state condition. It is suitable for developing dissimilar metal joints without introducing unwanted phases or microstructure at the bimetallic interface. It is known that multiple reactions occur for powder particles during SPS process: (1) plasma heating, (2) joule heating, and (3) uniaxial compression. Powder gets solidified and grain growth starts above recrystallization temperature of powder material. Since SPS is run under a solid-state diffusion mechanism, phase transformation may be accompanied.

This study used Thermal Technology LLC's SPS machine under industrial argon gas from Airgas Co. Sintering die radius was 20 mm radius and two different powders were sintered simultaneously. SPS sintering temperature varied by 800 ~ 1200 °C and isothermal dwell time was 16 minutes for each run. Uniaxial pressure rate was 20 MPa/min, and chamber vacuum condition was near ~ 18 torr. Fig. 1 illustrates the powder consolidation processes for Inconel 718 and 316L stainless steel powders at the same time.

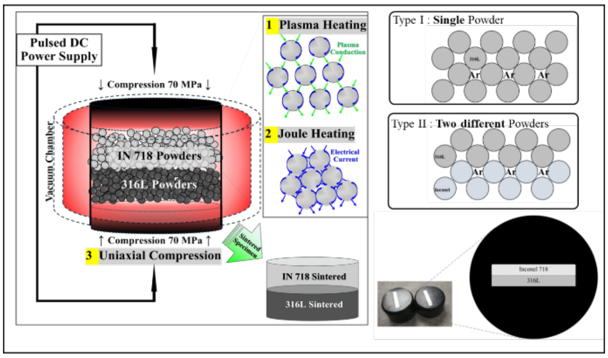

Fig. 1. Spark plasma sintering process and sintering material sample

2.3 Phase Availability between Alloy Systems

Table 2: Inconel 718 and 316L Phase composition

Inconel 718 and 316L available phases			
Alloy	**Phase**	**Crystal Structure**	**Chemical Formula**
Inconel 718	**γ**	FCC	Ni(Cr,Fe,Mo)
	γ'	FCC	$Ni_3(Al,Ti)$
	γ"	BCT	Ni_3Nb
	δ	Orthohrombic	Ni_3Nb
	σ	Tetragonal	(Cr,Mo)x (Ni,Co)y
	Laves Phase	Cubic / Hexagonal	$(Ni,Fe,Cr)_2(Nb,Ti,Mo)$
	MC	FCC	(Ti,Nb)C
	M23C6	FCC	$(Cr,Fe,Mo)_{23}C_6$
	M6C	Cubic / Hexagonal	Fe_3Mo_3C
316L	**γ (austenite)**	FCC	Fe Cr Ni Mo
	α', ε (martensite)	BCT, HCP	Fe Cr Ni Mo
	σ	Fe(CrMo) / tetragonal	Fe(CrMo)
	x (Chi)	BCC	$Fe_{36}Cr_{12}Mo_{10}$
	η (Laves)	Hexagonal	Fe_2Mo
	M23C6	$(FeCr)_{23}C_6$ / FCC	$(FeCr)_{23}C_6$

2.4 Grain Size Evolution

The grain size was reduced from non-sintered powder to the 900 °C SPSed sample. This reduction in grain size began to increase at 1000°C. Grain growth was more evident in 316L than in Inconel 718, as shown in **Fig. 2.** Grain growth was severe in 316L due to the distinct compositions and microstructural differences. For compositional reasons, Fe-based 316L promotes austenitic growth without any hindrance except minor oxide inclusion formations. However, for Inconel 718, the Nb element forms strengthening precipitates (γ' and γ") that inhibit grain growth. These precipitates form during heat treatment pin the grain boundaries, thus limiting the grain growth.

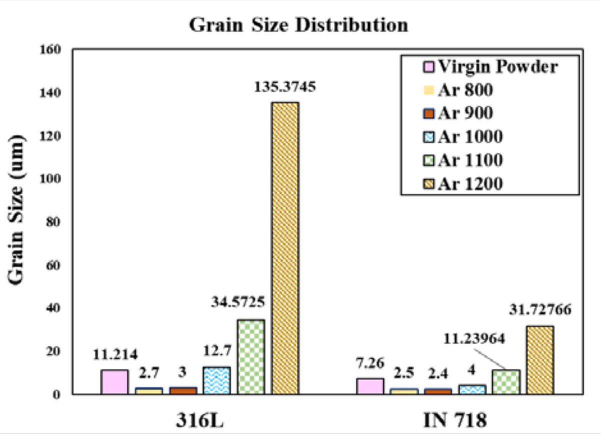

Fig. 2. Average grain size as a function of temperature.

2.5 Phase Evolution: Intermetallic and Precipitates

As shown in **Table 2**, the major elements in both Inconel 718 and 316L are: nickel, iron and chromium which is also known as typical oxide forming agents. The minor elements (Nb, Mo, Ti) are conventional nitride forming agents based on Ellingham's diagram. At sintering temperature higher than 1000 °C showing porosity less than 2%, the notable Laves phase observed in the feedstock powder decreased. It assumes some of the Nb and Mo in the Laves phase dissolved back to the matrix. Interestingly, γ′ phase (Al-Ti rich) was mainly identified at the grain boundaries at the high temperature conditions.

2.6 Microstructural Evolution at Interface

The grain size has diminished from 800 °C to 900 °C since the original powder is from the virgin form (as atomized). This diminishment of grain size was notable at lower temperature which proves the 1000 °C is a grain growth temperature and interface stabilizing temperature – which will be demonstrate by pole figure and inverse pole figure data. Particle-to-particle boundaries and grain boundaries have difference in minor element content since the vacancy between particle-to-particle boundaries was critical of formation of intermetallic compounds and precipitates.

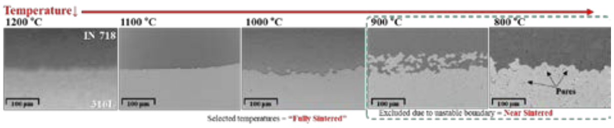

Fig. 4. Interface evolution via temperature diminishment

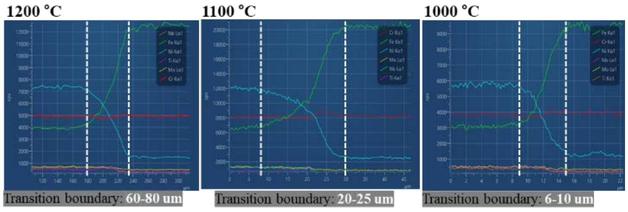

Fig. 5. Interface boundary profile from temp 1200, 1100 and 1000 °C

The uniform interface was fully formed above 1000 °C. From a particle's perspective, the interface was loaded with large amount of heat and pressure and grain growth of both 316L, and Inconel 718's minor elements were migrated. Thus, the interdiffusion in elements of both alloys can diffuse across the interface leading to the formation of mixture-precipitation of both phases.

4. Conclusions

The microstructure of Inconel 718 and 316L alloys and the interface underwent significant alterations at elevated SPS temperature. As the temperature increased, the interface boundary between the alloys became more pronounced, and the depth of the mixing region expanded correspondingly. The stability of the interface is influenced by the diffusion of elements from each alloy to the opposite side. The intermetallic network, particularly the Nb-Mo length, exhibited an increase, demonstrating the reduction of the stable Laves phase and the formation of new precipitated phases (γ') at elevated temperatures.

REFERENCES

[1] E. Hosseini, V.A. Popovich, A review of mechanical properties of additively manufactured Inconel 718, Addit. Manuf. 30 (2019). ARTN 100877 10.1016/j.addma.2019.100877.

[2] T.S. Byun, K. Farrell, Tensile properties of Inconel 718 after low temperature neutron irradiation, Journal of Nuclear Materials 318 (2003) 292-299. 10.1016/S0022-3115(03)00006-0.

[3] G.H. Lee, M. Park, B. Kim, J.B. Jeon, S. Noh, B.J. Kim, Evaluation of precipitation phase and mechanical properties according to aging heat treatment temperature of Inconel 718, J Mater Res Technol 27 (2023) 4157-4168. 10.1016/j.jmrt.2023.10.196.

[4] X. Li, J.J. Shi, C.H. Wang, G.H. Cao, A.M. Russell, Z.J. Zhou, C.P. Li, G.F. Chen, Effect of heat treatment on microstructure evolution of Inconel 718 alloy fabricated by selective laser melting, J. Alloy Compd. 764 (2018) 639-649. 10.1016/j.jallcom.2018.06.112.

[5] I.A. Segura, J. Mireles, D. Bermudez, C.A. Terrazas, L.E. Murr, K. Li, V.S.Y. Injeti, R.D.K. Misra, R.B. Wicker, Characterization and mechanical properties of cladded stainless steel 316L with nuclear applications fabricated using electron beam melting, Journal of Nuclear Materials 507 (2018) 164-176. 10.1016/j.jnucmat.2018.04.026.

[6] Y. Zhong, L.E. Rännar, L.F. Liu, A. Koptyug, S. Wikman, J. Olsen, D.Q. Cui, Z.J. Shen, Additive manufacturing of 316L stainless steel by electron beam melting for nuclear fusion applications, Journal of Nuclear Materials 486 (2017) 234-245. 10.1016/j.jnucmat.2016.12.042.

[7] T.S. Byun, B.E. Garrison, M.R. McAlister, X. Chen, M.N. Gussev, T.G. Lach, A. Le Coq, K. Linton, C.B. Joslin, J.K. Carver, F.A. List, R.R. Dehoff, K.A. Terrani, Mechanical behavior of additively manufactured and wrought 316L stainless steels before and after neutron irradiation, Journal of Nuclear Materials 548 (2021). ARTN 152849
10.1016/j.jnucmat.2021.152849.

[8] K.L. Murty, I. Charit, Structural materials for Gen-IV nuclear reactors: Challenges and opportunities, Journal of Nuclear Materials 383 (2008) 189-195. 10.1016/j.jnucmat.2008.08.044.

[9] G. Locatelli, M. Mancini, N. Todeschini, Generation IV nuclear reactors: Current status and future prospects, Energ Policy 61 (2013) 1503-1520. 10.1016/j.enpol.2013.06.101.

[10] A. Hinojos, J. Mireles, A. Reichardt, P. Frigola, P. Hosemann, L.E. Murr, R.B. Wicker, Joining of Inconel 718 and 316 Stainless Steel using electron beam melting additive manufacturing technology, Mater Design 94 (2016) 17-27. 10.1016/j.matdes.2016.01.041.